BRAIN COMMUNICATIONS

EphB3 interacts with initiator caspases and FHL-2 to activate dependence receptor cell death in oligodendrocytes after brain injury

Yanina Tsenkina,* Stephen A. Tapanes,* Madelen M. Díaz, David J. Titus, Shyam Gajavelli, Ross Bullock, Coleen M. Atkins and Daniel J. Liebl

These authors contributed equally to this work.

Clinical trials examining neuroprotective strategies after brain injury, including those targeting cell death mechanisms, have been underwhelming. This may be in part due to an incomplete understanding of the signalling mechanisms that induce cell death after traumatic brain injury. The recent identification of a new family of death receptors that initiate pro-cell death signals in the absence of their ligand, called dependence receptors, provides new insight into the factors that contribute to brain injury. Here, we show that blocking the dependence receptor signalling of EphB3 improves oligodendrocyte cell survival in a murine controlled cortical impact injury model, which leads to improved myelin sparing, axonal conductance and behavioural recovery. EphB3 also functions as a cysteine-aspartic protease substrate, where the recruitment of injury-dependent adaptor protein Dral/FHL-2 together with caspase-8 or -9 leads to EphB3 cleavage to initiate cell death signals in murine and human traumatic brain-injured patients, supporting a conserved mechanism of cell death. These pro-apoptotic responses can be blocked via exogenous ephrinB3 ligand administration leading to improved oligodendrocyte survival. In short, our findings identify a novel mechanism of oligodendrocyte cell death in the traumatically injured brain that may reflect an important neuroprotective strategy in patients.

The Miami Project to Cure Paralysis, Department of Neurosurgery, University of Miami Miller School of Medicine, Miami, FL, USA

Correspondence to: Daniel J. Liebl, PhD, Professor of Neurological Surgery, The Miami Project to Cure Paralysis, The University of Miami, 1095 NW 14th Terrace, R-48, Miami, FL 33136, USA
E-mail: dliebl@miami.edu

Keywords: traumatic brain injury; dependence receptors; cell death; oligodendrocytes; EphB3

Abbreviations: CAPs = compound action potentials; CCIcontrolled cortical impact; CNScentral nervous system; dpi = days post-injury; EdU = 5-ethynyl-2′-deoxyuridine; EM = electron microscopy; GFP = green fluorescent protein; hpi = hours post-injury; IP = immunoprecipitation; N1 = short-latency, fast-conducting myelinated axons; N2 = long-latency, slow-conducting unmyelinated axons; OLs = oligodendrocytes; OPC = oligodendrocyte progenitor cell; PBS = phosphate-buffered saline; PLP = proteolipid protein; TBI = traumatic brain injury; WT = wild type

Received February 4, 2020. Revised September 9, 2020. Accepted September 17, 2020. Advance Access publication October 18, 2020

Graphical Abstract

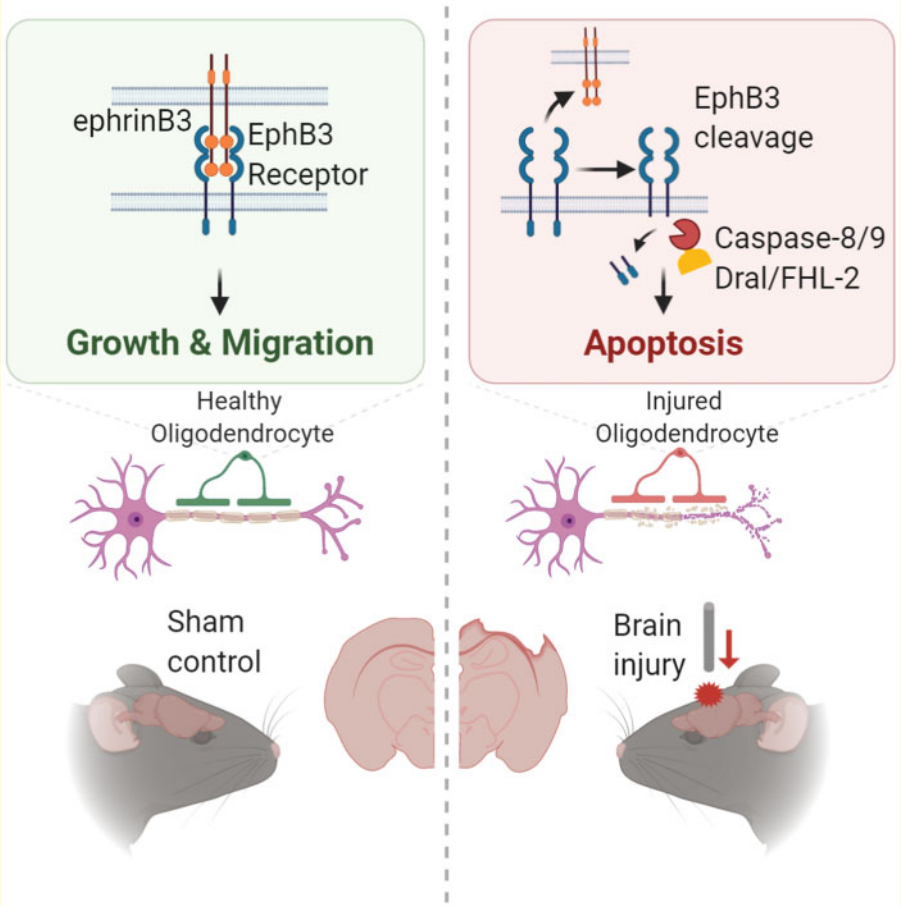

Introduction

According to the World Health Organization, by the year 2020 traumatic brain injury (TBI) will surpass many diseases to become the leading cause of patient death and disability worldwide (World Health Organization, 2018). Patients at risk for prolonged neurological deficits have significant underlying pathology that results from both the initial insult and progressive secondary damage. Cellular apoptosis, axonal damage and demyelination, synaptic damage and inflammation all contribute to the secondary injury and represent therapeutic targets for minimizing injury progression.

The tumour necrosis factor receptor superfamily comprising the tumour necrosis factor receptor 1, death receptors 3–6 and CD95 (FAS) receptor are plasma membrane proteins that contain death domains and are believed to be key initiators of pro-apoptotic signals in the injured brain (Ashkenazi and Dixit, 1998; Casha *et al.*, 2001). Upon ligand activation, these classical 'death' receptors activate downstream caspase signalling pathways that can lead to cellular apoptosis. Unfortunately, clinical trials targeting members of this family have been largely unsuccessful (Shohami *et al.*, 1999; Narayan *et al.*, 2002; Xiong et al., 2009; Loane and Faden, 2010; Kabadi and Faden, 2014). One explanation for this failure could be the existence of other pro-apoptotic initiators in the injured brain. In cancer biology, a new family of death receptors has emerged where pro-apoptotic signalling occurs in the absence of ligand stimulation (Mehlen *et al.*, 1998; Mehlen and Bredesen, 2004; Goldschneider and Mehlen, 2010). This atypical receptor-mediated transduction response can be blocked upon ligand interactions, thus creating a dependence (or addiction) on its respective ligand. This new family of death receptors has been classified as dependence receptors, where alterations in ligand and/or receptor expression levels or coupling are thought to have significant implications on tumour formation and growth (Mehlen and Bredesen, 2004; Tauszig-Delamasure *et al.*, 2007; Goldschneider and Mehlen, 2010). To date, there are >20 identified dependence receptors that can be differentially activated in the absence of their ligands that in part include members of the ephrin, netrin-1, insulin, semaphorin and neutrophin receptor families (Mehlen *et al.*, 1998; Llambi *et al.*, 2001; Mehlen and Bredesen, 2004; Llambi *et al.*, 2005; Bredesen *et al.*, 2006; Tauszig-Delamasure *et al.*, 2007; Furne *et al.*, 2009;

Goldschneider and Mehlen, 2010; Theus *et al.*, 2014; Tsenkina *et al.*, 2015). Recently, we have discovered that a specific member of the dependence receptor family, namely the EphB3 receptor, plays critical roles in cell death after traumatic central nervous system (CNS) injury (Theus *et al.*, 2014; Tsenkina *et al.*, 2015; Assis-Nascimento *et al.*, 2018).

EphB3 is activated by membrane-bound ephrin ligands that can lead to bidirectional signalling, which emphasizes the importance of cell–cell interactions in mediating ligand–receptor signalling (Himanen *et al.*, 2007; Nikolov *et al.*, 2013). In TBI, acute cellular disruption leads to cell dissociation and provides the framework for non-ligated Ephs to initiate dependence-mediated cell death mechanisms. We have recently begun to implicate EphB3 in TBI-induced cell death where improved cell survival is observed in genetically ablated mice or following administration of the ligand ephrinB3 (Theus *et al.*, 2014; Assis-Nascimento *et al.*, 2018). Two highly susceptible cells to TBI-mediated cell death are neurons and myelin-producing oligodendrocytes (OLs), where significant losses can contribute to many of the observed functional deficits (Clark *et al.*, 2001; Knoblach *et al.*, 2004; Slemmer *et al.*, 2008; Lotocki *et al.*, 2011; Flygt *et al.*, 2013; Sullivan *et al.*, 2013; Dent *et al.*, 2015; Mierzwa *et al.*, 2015). Although there is a great deal known about neuronal cell death mechanisms, fewer studies have examined OL cell death. OLs play a critical role in maintaining axonal health and functional activity, where pathological demylination and axonal degeneration underlie a majority of the functional losses associated with TBI (Levin *et al.*, 1990; Bigler *et al.*, 1994; Bramlett and Dietrich, 2002). OL losses have been reported to occur as early as 4 h post-injury (hpi) in human TBI patients (Flygt *et al.*, 2016), and have been associated with axonal damage and other white matter pathologies in both human patients (Johnson *et al.*, 2013) and animal models of TBI (Sullivan *et al.*, 2013; Mierzwa *et al.*, 2015). The present study examines the temporospatial dynamics of EphB3-mediated cell death in OLs, the mechanisms of action and the cellular and functional responses to neutralizing EphB3 pro-apoptotic signalling after brain injury in mice.

Materials and methods

Animals

Male C57Bl/6 wild type (WT), proteolipid protein (PLP)–green fluorescent protein (GFP) (Fuss *et al.*, 2000) and EphB3 knockout ($EphB3^{-/-}$) mice (Orioli *et al.*, 1996) between 2 and 4 months of age were used for this study. The animals were kept under normal 12-h light/dark cycle conditions, and food/water was provided *ad libitum*. All animal procedures were approved by the University of Miami Animal Use and Care Committee.

Controlled cortical impact injury and ephrinB3 administration

Sham and controlled cortical impact (CCI)-injured animals were anaesthetized by intraperitoneal injection of ketamine (100 mg/kg) and xylazine (10 mg/kg). Following the craniotomy, the CCI injury was produced using a 3-mm bevelled piston attached to an eCCI-6.3 device (Custom Design & Fabrication, Virgina Commonwealth, VA, USA) at a velocity of 4 m/s, a depth of 0.55 mm and 150 ms impact dwell duration. Sham controls underwent an identical surgical procedure in the absence of the craniotomy and injury. Animals were caged in groups prior to surgery and caged individually during the recovery period.

For intracortical infusion, micro-osmotic pumps (Alzet, Durect Corp, Cupertino, CA, USA; model 1007D) assembled according to the manufacturer's recommendations were preloaded with purified ephrinB3 extracellular domain protein (ephrinB3; Nelersa *et al.*, 2012) at 100 µg/ml or vehicle [1× phosphate-buffered saline (PBS), pH 7.4]. For cell count studies, an infusion cannula was placed over the injury epicentre at the time of injury. EphrinB3 or vehicle compound were dispensed at a rate of 0.05 µg per hour over a 7-day infusion period (i.e. 1.2 µg/day). For cleavage studies, ephrinB3 and vehicle control were also administered via a combined tail vein intravenous (0.43 mg/kg) and intraperitoneal (2.17 mg/kg) injections 1 h after CCI injury, and the animals were sacrificed at 6 hpi.

Histology and immunohistochemistry

For *in situ* analysis, the animals were transcardially perfused with 4°C PBS (pH 7.4) followed by 4% paraformaldehyde (pH 7.4), postfixed in 4% paraformaldehyde overnight at 4°C and then transferred to 30% sucrose in PBS solution. The brains were embedded in Tissue-Tek OCT solution (Sakura, Torrance, CA, USA) and frozen with isopentane. Thirty-micron thick sections were serially cut using a cryostat and immunoreacted as previously described (Perez *et al.*, 2016; Assis-Nascimento *et al.*, 2018).

Stereology

Tissue samples were prepared as described above and stereological counts were performed as previously described using a motorized Olympus BX51TRF microscope, Optronix cooled video camera and MicroBrightField StereoInvestigator software package (MBF Bioscience, Williston, VT, USA) (Tsenkina *et al.*, 2015). Nonbiased 'blinded' cell number evaluation was performed by means of the optical fractionator method and the optical dissector probe. White and grey matter regions of interest in the ipsilateral hemisphere (depicted in Fig. 1) were manually traced with contours using 5× magnification. Subsequently, a grid of 200 × 200 μm^2 was placed over the selected area and immunopositive

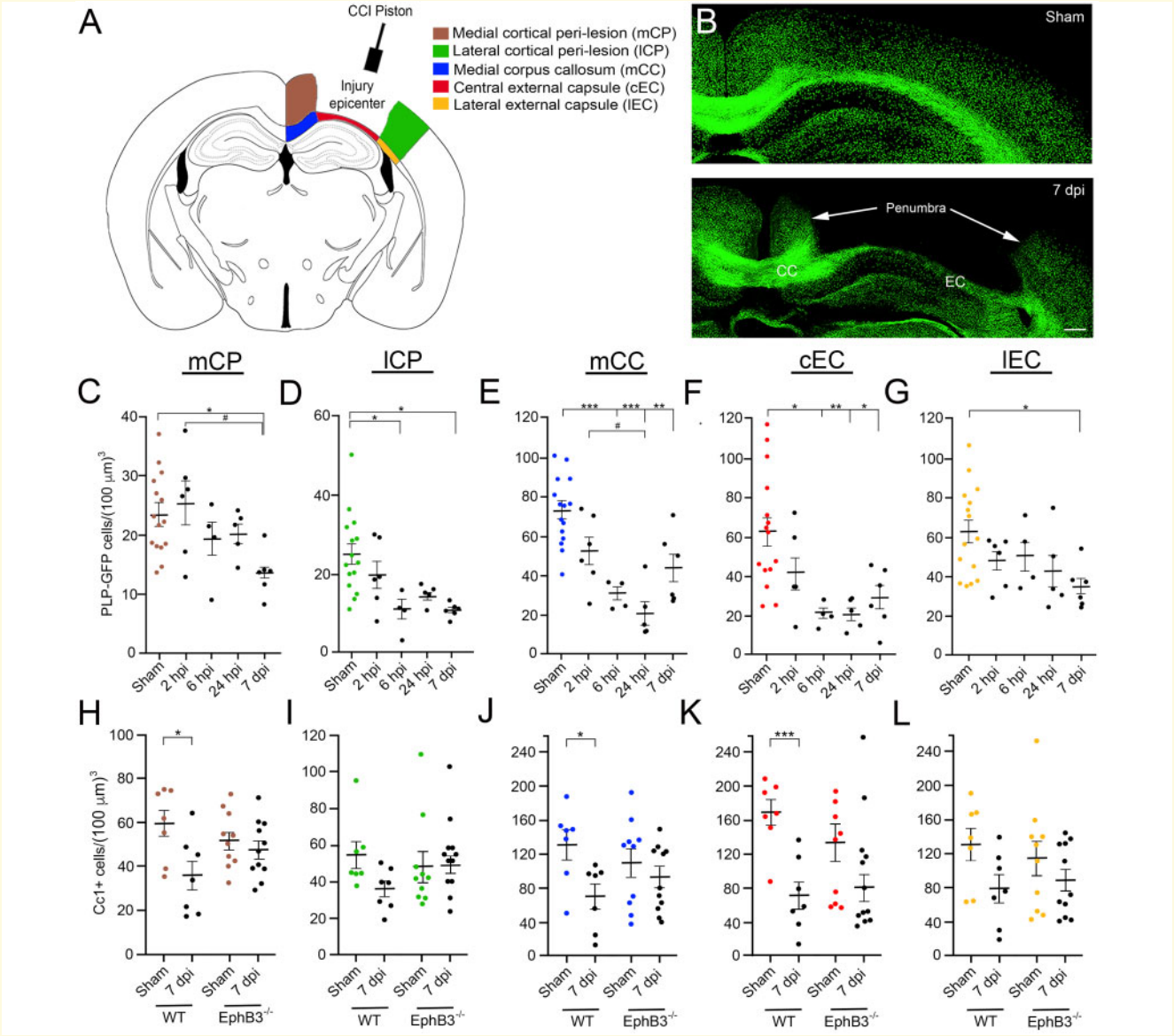

Figure 1 Temporospatial losses in OLs are region specific after CCI injury and are reduced in the absence of EphB3. (**A**) Schematic representation of the cortical grey matter and white matter tracts being evaluated in CCI-injured and sham brain between 2 hpi and 7 dpi. Colour mapping coordinates to panels (**C**)–(**L**), and sham tissue map to similar regions. (**B**) Representative images of PLP–GFP mice where GFP-labeled OLs are observed in sham and 7 dpi brains. Bar represents 400 µm. Stereological counts of GFP-labeled OLs in sham, 2 hpi, 6 hpi, 24 hpi and 7 dpi within the mCP (**C**), ICP (**D**), mCC (**E**) cEC (**F**) and lEC (**G**). Stereological counts of anti-Cc1-labeled OLs were examined in the mCP (**H**), ICP (**I**), mCC (**J**), cEC (**K**) and lEC (**L**) in WT and EphB3$^{-/-}$ mice. *n*-Values were between 5 and 15/group. $^{*,\#}P < 0.05$; $^{**}P < 0.01$; $^{***}P < 0.001$. Values are presented as mean ± SEM. cEC = central external capsule; ICP = lateral cortical peri-lesion; lEC = lateral external capsule; mCC = medial corpus callosum; mCP = medial cortical peri-lesion.

cells were counted using an optical fractionator at 63× (sampling box 50 × 50 µm^2) at 2 hpi, 6 hpi, 24 hpi and/or 7 days post-injury (dpi) (Supplementary Fig. 1A and B).

5-Ethynyl-2′-deoxyuridine administration and immunostaining

WT and EphB3$^{-/-}$ mice were administered 50 mg/kg of 5-ethynyl-2′-deoxyuridine (EdU; Invitrogen) at 1 and 3 dpi. The animals were sacrificed at 7 dpi. Cryosectioned tissues were stained with a Click-iT EdU Imaging Kits (Invitrogen) following manufacturer's instructions, and cells were counted using a standard stereological approach (Assis-Nascimento *et al.*, 2018).

Protein assay and immunoprecipitation

The ipsilateral cortex and underlying white matter around the injury epicentre were dissected at 2 hpi, 6

hpi, 24 hpi, 7 dpi and sham mice. Brain lysates (30 µg) were prepared and resolved in 10% sodium dodecyl sulfate-polyacrylamide gels as previously described (Theus *et al.*, 2014). The primary mouse anti-EphB3 (Novus Abnova, Littleton, CO, USA), anti-caspase-3 and cleaved caspase-3 (Cell Signaling, Danvers, MA, USA), anti-caspase-8 and cleaved caspase-8 (Cell Signaling), anti-caspase-9 and cleaved caspase-9 (Abcam, Cambridge, MA, USA) or anti-FHL-2 (Abcam) antibody were applied at 1:200 dilution in 5% bovine serum albumin solution overnight at 4°C. Protein expression was normalized to *β*-actin (Cell Signaling).

For IP, 150 µg of protein sample was incubated with 1.5 µg of anti-EphB3 IgG2a mouse antibody (Novus Abnova) or a negative mouse mAb IgG2a isotype control (Cell Signaling). The membrane was subsequently incubated with the primary antibody of interest (anti-EphB3, anti-caspase-3, -8 and -9 and anti-FHL-2).

Open field test

All mice were pre-handled and tested on an open field task for 10-min interval starting at 5 or 12 dpi in a plexiglass box (43.2-cm width, 43.2-cm length, 30.5-cm height) with transparent walls and a white floor. The animals' behaviour was automatically recorded using an Ultra 720+ Resolution DSP, True Day/Night Color camera (Everfocus, Duarte, CA, USA) and analysed using EthoVision XT Version 10.0 software (Noldus, Asheville, NC, USA). The mouse's movements (speed and distance travelled) were automatically recorded blinded.

Electron microscopy

WT and EphB3$^{-/-}$ sham and injured animals were perfused with cold PBS followed by 2% glutaraldehyde–2% paraformaldehyde fixative in 0.1 M phosphate buffer and postfixed with 3% electron microscopy (EM) grade glutaraldehyde. Using a Philips CM-10, 15 non-overlapping randomized images were taken at 7900 magnification per sample throughout the area of interest. Myelin thickness and axon diameter were measured in a blinded fashion on five EM images for each animal using ImageJ software and the G-ratio was calculated as a ratio (the axon/axon + myelin). In addition, compact myelinated, loosely myelinated, collapsed axons/myelinated and unmyelinated axons were evaluated on 15 EM images per animal.

Compound action potential electrophysiology

At 7 dpi, corpus callosum compound action potential (CAP) recordings were performed blinded as previously described (Reeves *et al.*, 2005; Crawford *et al.*, 2009). Under deep anaesthesia (3% isoflurane, 70% N_2O, 30% O_2, 2 min), the animal was decapitated and the brain was rapidly removed. Coronal slices (400 µm) were prepared with a vibratome (Leica Biosystems, Buffalo Grove, IL, USA) in ice-cold artificial cerebrospinal fluid: 124 mM NaCl, 5 mM KCl, 1.25 mM NaH_2PO_4, 26 mM $NaHCO_3$, 1.3 mM $MgSO_4$, 2 mM $CaCl_2$ and 10 mM glucose, saturated with 95% O_2/5% CO_2. CAPs were evoked by stimulating the CC with a platinum-iridium concentric bipolar electrode and evoked CAPs were recorded with a glass electrode filled with 2 M NaCl (1–3 MΩ) using a Multiclamp 700B amplifier and pClamp 10.4 software (Molecular Devices, Sunnyvale, CA, USA). The stimulating electrode was placed 0.5-mm lateral to midline on the contralateral side and the recording electrode was placed 1.0 mm from the stimulating electrode on the ipsilateral side. Recordings were low-pass filtered at 2 kHz and digitized at 20 kHz (Digidata 1440A; Molecular Devices). Input–output curves were obtained by increasing the stimulus intensity at 0.2 mA steps (200 µs duration, delivered at 0.1 Hz) until the—CAP reached asymptomatic maximum. The amplitude of the CAP waveforms (N_1 and N_2) were measured. Conduction velocity was determined by altering the distance between the stimulating and recording electrodes from 0.5 to 2 mm and measuring the peak latency of the N_1 and N_2 CAP components.

Human brain tissue collection

The collection of human TBI brain tissues was approved by the University of Miami Institutional Review Board (protocol # 20030154 and 20080609), and informed consent was obtained for each patient.

HEK293T cell cultures

Human kidney embryonic cells (HEK293T) were cultured as previously described (Theus *et al.*, 2014). For transient transfection, we used 2 µg pcDNA3.1-V5, pcDNA3.1-V5-EphB3^{FL}, pcDNA3.1-V5-EphB3^{D849N}, pcDNA3.1-V5-EphB3$^{1-849}$, pcDNA3.0 DH5α Caspase-9^{DN} and/or 100 nM Dral/FHL-2 siRNA (Thermo Fischer) and Cy3-labeled negative control siRNA (Thermo Fischer) following manufacturer's recommendations (Polyplus-transfection, New York, NY, USA). After transfection, cellular stress was induced 1 day later through serum deprivation. For some experiments, 1 µg/ml ephrinB3 or vehicle control was added every 12 h. Cell viability was assessed 24 h following serum deprivation by means of a trypan blue exclusion assay (Sigma) and automated cell counting (Bio-Rad, Hercules, CA, USA). For the western blot analysis of EphB3 receptor cleavage, cells were serum starved for 4 h and proteins were extracted using standard procedures for the western blot assay. IP of EphB3 receptor with caspase-9 in the absence or presence of Dral/FHL-2, ephrinB3 and/or vehicle was examined 30 min after serum deprivation using the standard procedures.

Oligodendrocyte progenitor cell culturing, transfection and viability assay

Primary oligodendrocyte progenitor cells (OPCs) were grown from frozen stocks and cultured at a seeding density of 2×10^6 cells/well as previously described (Tsenkina *et al.*, 2015). For transfection, OPCs were plated in a six-well plate at a density of 5×10^4 cells/well and grown for 24 h to reaching 70–80% confluency. OPCs were then transfected with 50 nM of Cy3-labeled scramble siRNA or 50 nM FHL-2 siRNA (Ambion) using JetPrime Reagent (PolyPlus) according to the manufacturer's recommendations and verified using Cy3 fluorescence and western blot analysis of FHL-2 expression. A complete media change was performed after 24 h to halt transfection and OPCs were cultured for 48 h. OPCs were subjected to 10 nM staurosporine (Cell Signaling) or vehicle for 48 h to induce cellular stress as previously described (Tsenkina *et al.*, 2015).

Statistical analysis

Statistical comparisons were performed using GraphPad Prism software, Version 4 (GraphPad Software, Inc., San Diego, CA, USA). Data meeting the normality assumption were analysed using Student's two-tailed *t*-test for the comparison of two experimental groups, or a one-way or two-way ANOVA for the comparison of more than two groups with Tukey's *post hoc* correction. Correlations were performed using Pearson's analysis.

Data availability

The authors confirm that all data within this article are readily available upon request.

Results

Temporospatial loss of OL cells after CCI injury

To examine the temporospatial pattern of surviving OLs following murine CCI injury, we examined regional damage in the cortical peri-lesion and underlying white matter tracts between 2 hpi and 7 dpi (Fig. 1A). Colour coding was used to facilitate differentiation between five regions, including the medial cortical peri-lesion (brown) and lateral cortical peri-lesion (green), medial corpus callosum (blue), the central external capsule (red) that is under the injury epicentre and the lateral external capsule (yellow) (Fig. 1A). The number of surviving GFP-labeled cells in the grey and white matter was counted in sham and CCI-injured mice expressing GFP driven by the PLP promoter (i.e. PLP–GFP mice), where Fig. 1B depicts a representative sham and 7 dpi brain section. In the medial cortical peri-lesion, significant losses in OLs were observed at 7 dpi (~50%) as compared to sham mice and 2 hpi, but not in the first day post-injury (Fig. 1C). Alternatively, the lateral cortical peri-lesion showed significant OL losses by 6 hpi that were maintained throughout 7 dpi (Fig. 1D). In the underlying white matter tracts, the medial corpus callosum and central external capsule showed rapid OL losses that were maximal by 6–24 hpi as compared to sham mice (Fig. 1E and F). In the lateral external capsule, OL losses were not significant until 7 dpi (Fig. 1G).

Absence of EphB3 receptor improves OL survival

We have previously implicated dependence receptors in mediating cell death after CNS injury (Furne *et al.*, 2009; Theus *et al.*, 2014; Tsenkina *et al.*, 2015; Assis-Nascimento *et al.*, 2018) but have not examined the role of EphB3 on OL survival after TBI. To evaluate whether eliminating EphB3 is neuroprotective for OLs following CCI injury, we quantified Cc1-labeled OLs in WT and homozygous EphB3 deficient ($EphB3^{-/-}$) mice at 7 dpi as compared to sham controls (Fig. 1H–L). Significant deficiencies observed in WT OLs at 7 dpi were not observed in $EphB3^{-/-}$ OLs. These observations support a pro-cell death role for EphB3 but also suggest that EphB3 functions may have a generalized, although graded effect in all regions tested. We also examined whether the numbers of mature OLs at 7 dpi represented surviving OLs or an expansion of OPCs generating new OLs (Supplementary Fig. 1B–D). Animals were injected with EdU at 1 and 3 dpi and the number of EdU-/PLP–GFP-labeled OLs was quantified in the medial corpus callosum and central external capsule at 7 dpi. We observed no significant difference in the numbers of EdU-labeled OLs between WT sham and CCI-injured mice at 7 dpi (Supplementary Fig. 1B), suggesting that OPC differentiation does not significantly impact the numbers of OLs in the first week post-injury. We did observe a ~3-fold increase in the number of EdU-labeled cells in the CCI-injured white matter as compared to sham controls, but no differences were observed between WT and $EphB3^{-/-}$ animals (Supplementary Fig. 1C and D).

EphrinB3 administration blocks OL cell death after CCI injury

Dependence receptors are defined as receptors that activate pro-cell death signals in the absence of their respective ligand(s). To provide evidence that EphB3 functions as a dependence receptor in OL after CCI injury, intraventricular administration of 1.2 µg/day recombinant ephrinB3 protein was delivered via osmotic pumps starting at the time of injury to block Eph-mediated cell death, and then OL cell numbers were examined at 7 dpi. Stereological analysis of OLs in PLP–GFP mice showed

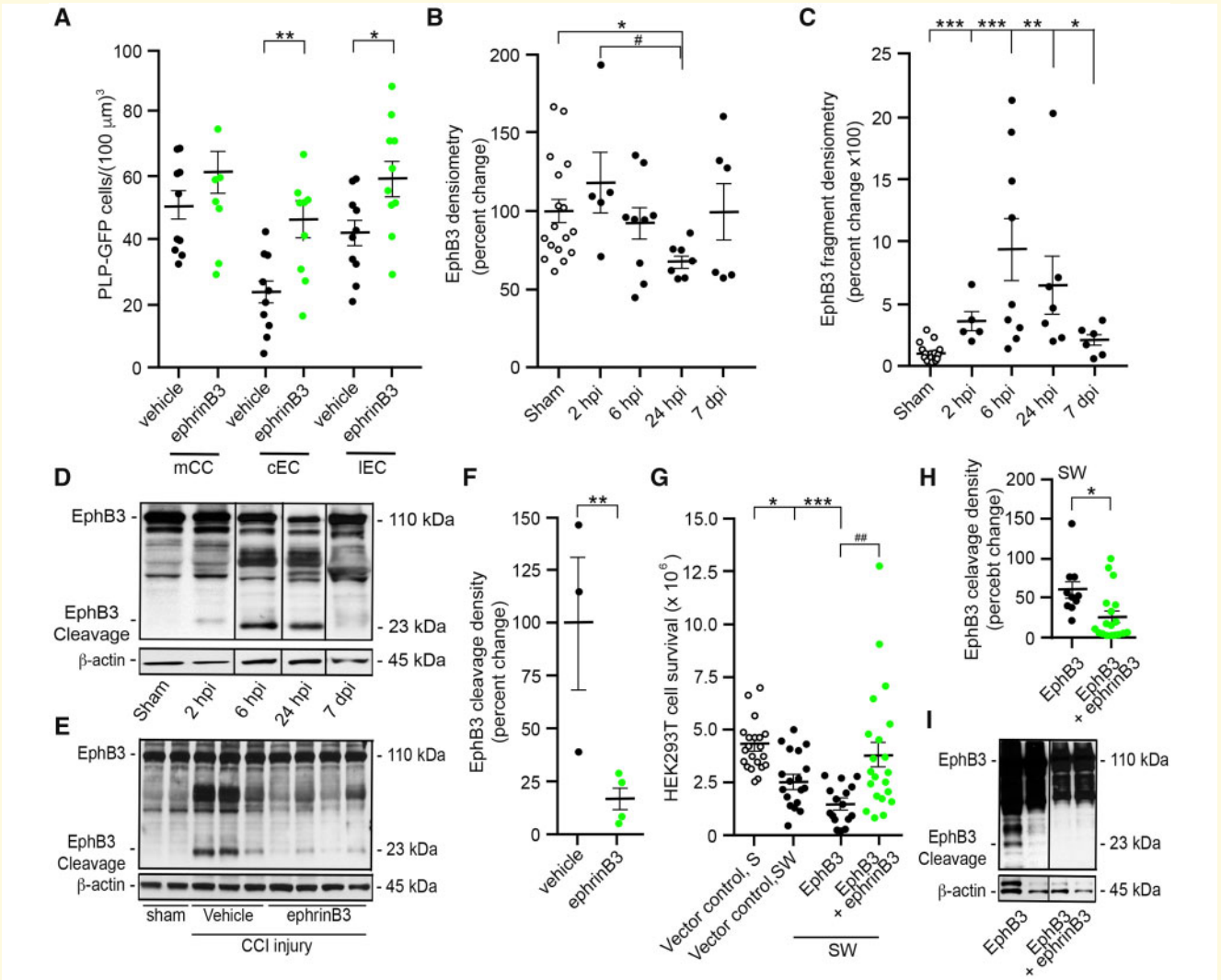

Figure 2 EphB3 receptor cleavage coincides with peak OL cell death and ephrinB3 administration prevents receptor cleavage and promotes cell survival. (**A**) Stereological counts of GFP-labeled OLs in the mCC, cEC and lEC at 7 dpi. *n*-Values were 10/group. Densitometry of EphB3 (**B** and **D**) and EphB3 cleavage product (**C** and **D**) in sham and CCI-injured mouse cortex at 2 hpi to 7 dpi. (**D**) Representative western blot. *n*-Values were between 5 and 17/group. Western blot (**E**) and densitometry (**F**) of EphB3 and cleaved EphB3 at 6 hpi following treatment with recombinant ephrinB3. (**G**) EphB3-transfected HEK293T cells undergo increased cell death as compared to control vector-transfected cells following SW, where ephrinB3 treatment reversed cell death (**G**) and EphB3 cleavage (**H** and **I**). *n*-Values were six biological replicates (16–21 technical replicates/group). (**I**) Representative western blot. $*^{\#}P < 0.05$; $**P < 0.01$; $***P < 0.0001$. Values are presented as mean ± SEM. cEC = central external capsule; lEC = lateral external capsule; mCC = medial corpus callosum; SW = serum withdraw.

greater numbers of surviving OLs in the white matter tracts of ephrinB3-treated CCI-injured mice as compared with vehicle (PBS)-treated CCI-injured mice (Fig. 2A). Specifically, we observed a significant increase in OL survival in the central external capsule and lateral external capsule regions.

TBI leads to EphB3 receptor cleavage

To further evaluate the dependence receptor role of EphB3 in the traumatically injured brain, we examined EphB3 cleavage using a C-terminal anti-EphB3 antibody (Supplementary Figs 1E and 2) in sham and CCI-injured cortical tissues. We observed little change in 110-kDa full-length EphB3 in the first 6 hpi; however, by 24 hpi EphB3 protein levels were reduced 25% as compared to sham controls (Fig. 2B and D and Supplementary Fig. 2). Consistent with previous findings, EphB3 protein levels in the injured brain returned to baseline by 7 dpi (Tsenkina *et al.*, 2015). Conversely, the ~23-kDa EphB3 cleavage product was observed as early as 2 hpi, peaked by 6 hpi and remained elevated for the entire 7 dpi as compared to sham controls (Fig. 2C and D and Supplementary Fig. 2). These findings

demonstrate that EphB3 cleavage directly precedes OL cell death and further implicates EphB3 in dependence receptor-mediated OL losses after TBI.

We next examined EphB3 cleavage following ephrinB3 administration, where an intravenous injection (0.4 mg/kg-body weight) and an intraperitoneal injection (2.0 mg/kg-body weight) of ephrinB3 (Nelersa *et al.*, 2012) were given to the same animals at 1 hpi, followed by tissue analysis at 6 hpi. We observed a significant reduction (83%) in EphB3 cleavage in the CCI-injured brain when ephrinB3 was systemically administered (Fig. 2E and F and Supplementary Fig. 2), supporting the possibility that improved OL survival following ephrinB3 administration is the direct result of blocking EphB3 cleavage. To further support this conclusion, we examined EphB3-mediated cell death in HEK293T cells overexpressing full-length EphB3 receptor. Transfection of EphB3 led to a significant reduction in HEK293T cell survival following serum withdrawal-induced cellular stress, which was reversed when cells were cultured in the presence of recombinant 1.0 µg/ml ephrinB3 (Fig. 2G). Examination of EphB3 cleavage in EphB3-transfected HEK293T cells showed a similar profile to cell death, where EphB3 cleavage was reduced in ephrinB3-treated cells (Fig. 2H and I and Supplementary Fig. 2).

We then examined the expression of full-length and cleaved EphB3 in cortical tissues from human TBI patients. Although fresh human TBI tissue samples are difficult to collect and have very little material to analyze, we obtained cortical samples from TBI patients ($n = 4$) at acute post-injury periods between 3 and 17.5 h after admittance to the hospital and compared them to non-injured control patients ($n = 3$) (Supplementary Fig. 1F and G). Control cortical tissues were obtained from patients who succumbed to heart failure and did not have brain trauma. We observed full-length EphB3 expression in all controls and 3 of 4 TBI patients, while cleavage fragments were observed in 3 of 4 TBI patients (Supplementary Figs 1F and 2). Although the small n-values and the limited protein material from TBI patients preclude our ability to perform biological/technical replicates, these findings support the presence and cleavage of EphB3 in adult human TBI cortical tissues.

EphB3 serves as a substrate for caspase-8 and -9, but not caspase-3

To examine the mechanisms that regulate EphB3 cleavage, we evaluated whether EphB3 functions as a caspase substrate using an IP approach at a time point prior to peak cleavage. EphB3 was immunoprecipitated with an anti-EphB3 antibody but not the IgG2a isotype control from sham and CCI injured mice at 2 hpi (Fig. 3A). The IP data showed that EphB3 associated with caspase-9 (Fig. 3B) and caspase-8 (Fig. 3C), but not caspase-3 (Fig. 3D). Analysis of total protein demonstrates that levels of cleaved caspase-8 and -9 were greater in CCI-injured tissues as compared to sham controls (Fig. 3B and C), although caspase-3 levels are consistent between the two groups at 2 hpi (Fig. 3D). It should be noted that because a C-terminal EphB3 antibody was used for IP, only the full-length, 'non-cleaved' EphB3 was detected at the 110-kDa band.

To determine whether tissue levels of the cleaved forms of caspase-8 and -9 paralleled the peak period for EphB3 cleavage after CCI injury, we examined pro- and cleaved-caspases between 2 hpi and 7 dpi (Fig. 4). We observed both pro- and cleaved-caspases in the injured cortex between 2 and 24 hpi (Fig. 4A–F and Supplementary Fig. 3). Conversely, caspase-3 levels remained constant (Fig. 4G–I). To examine whether caspase levels are dependent on the presence of EphB3 as a binding substrate, we measured caspase levels in WT and EphB3$^{-/-}$ cortices at 6 hpi (Fig. 4J–O). Significant increases were observed in both cleaved caspase-8 (Fig. 4K and L and Supplementary Fig. 3) and cleaved caspase-9 (Fig. 4M and O and Supplementary Fig. 3) levels in WT CCI-injured tissues but not in EphB3$^{-/-}$-injured tissues. No differences were observed between WT and EphB3$^{-/-}$ sham mice.

Since EphB3 cleavage primarily occurs in the CCI-injured brain, it suggests that other protein(s) may be required for caspase-mediated cleavage. For this reason we investigated whether the adaptor protein Dral/FHL-2 may be involved in EphB3-caspase-9 mediated cell death. We observed increased Dral/FHL-2 levels in CCI-injured cortices by 2 hpi, a time point prior to peak EphB3 cleavage (Fig. 5A and Supplementary Fig. 4). Interestingly, examination of human TBI tissues showed Dral/FHL-2 expression in 2 of the 4 TBI patients, but not in control tissues (Supplementary Figs 5A and 6), which corresponded to TBI patients with cleaved EphB3 (Supplementary Fig. 1F). We next examined whether Dral/FHL-2 associated with EphB3 in stressed primary OPCs and human embryonic kidney HEK293T cells. Primary cultured OPCs express both EphB3 and Dral/FHL-2 protein, and following 10 nM staurosporine stress, we observed that both caspase-9 and Dral/FHL-2 immunoprecipitated with EphB3 (Fig. 5B and Supplementary Fig. 4). We also performed siRNA knockdown experiments to determine whether reducing Dral/FHL-2 levels led to changes in OPC viability. OPCs were transfected with either 50 nM scrambled or Dral/FHL-2 siRNA and then stressed with 10 nM staurosporine. Dral/FHL-2 siRNA treatment led to a >60% reduction in Dral/FHL-2 protein levels (Supplementary Figs 5B and C and 6). Stress induced by transfection alone or both transfection and staurosporine treatment led to reduced OPC viability, which was significantly reversed in Dral/FHL-2 siRNA-treated cultures as compared to scrambled siRNA controls (Fig. 5C). In HEK293T cells, EphB3 over-expression did not lead to association with endogenous Dral/FHL-2 at 30 min after stress (Fig. 5D and Supplementary Fig. 4);

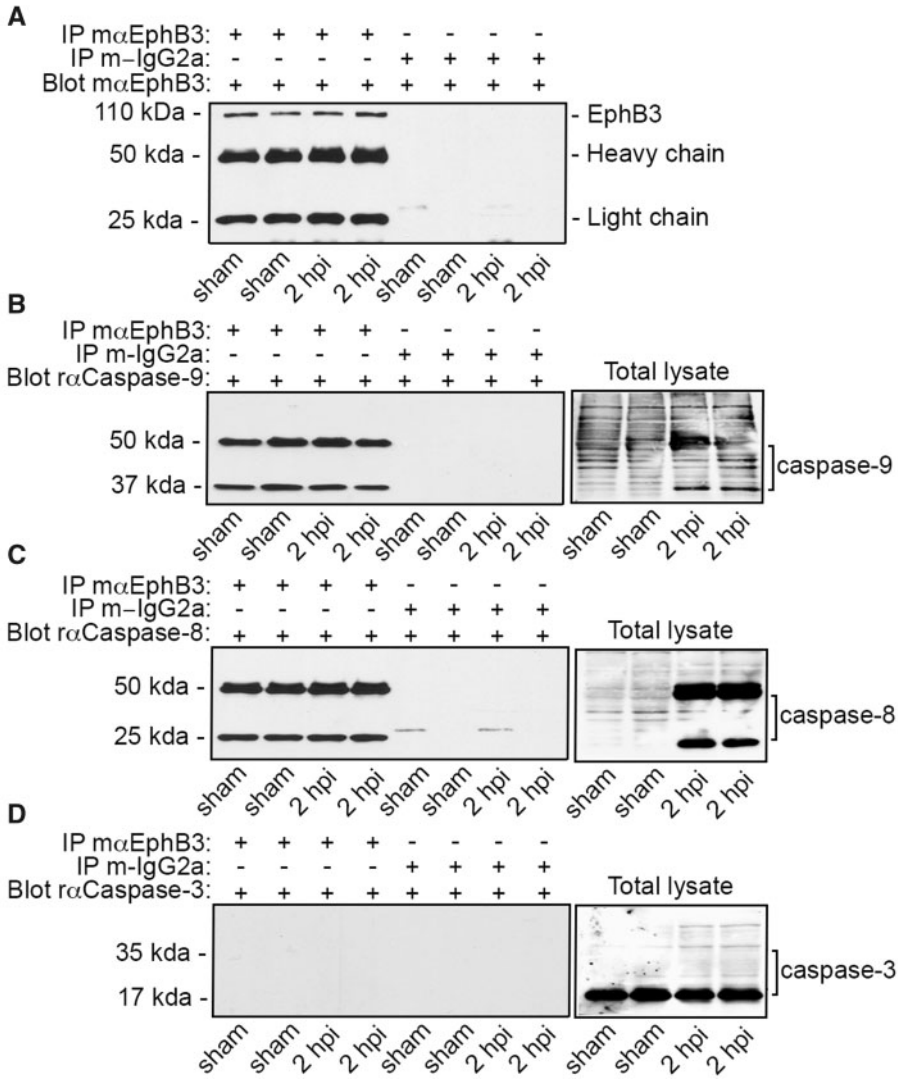

Figure 3 IP studies show that EphB3 associates with caspase-8 and -9 but not caspase-3. (**A**) EphB3 binds specifically to anti-EphB3 antibodies, but not an IgG2a control in both sham and 2 hpi tissues. (**B**) Caspase-9 immunoprecipitates with EphB3 in both sham and 2 hpi tissues, but not with control IgG2a samples. Total lysates show the up-regulation of cleaved caspase-9 after CCI injury. (**C**) Caspase-8 immunoprecipitates with EphB3 in both sham and 2 hpi tissues, but not with control IgG2a samples. Total lysates show the up-regulation of caspase-8 after CCI injury. (**D**) Caspase-3 does not immunoprecipitate with either EphB3 or IgG2a in sham and 2 hpi tissues. Total lysates show the presence of caspase-3 in sham and CCI-injured tissues. *n*-Values were sham and CCI injury, $n = 2$/group in duplicate. mα = mouse antibody; rα = rabbit antibody.

however, over-expression of both EphB3 and dominant-negative-caspase-9 resulted in the Dral/FHL-2 complex formation (Fig. 5E and Supplementary Fig. 4). It was important to employ a non-cleavable dominant-negative-caspase-9 to reduce the possibility of premature cell death from enhanced caspase activation that limited our ability to observe these protein interactions. This was supported by HEK293T IP studies at 2 h following stress where Dral/FHL-2 association with EphB3 was no longer observed, suggesting that competition of endogenous caspase-9 and dominant-negative-caspase-9 eventually led to cell death (not shown). We also transfected HEK293T cells with a non-cleavable form of EphB3 (i.e. $EphB3^{D849N}$), where the aspartate residue at amino acid 849 is replaced with an asparagine (Theus *et al.*, 2014), and observed no association of Dral/FHL-2 with $EphB3^{D849N}$ at 2 h following stress (Supplementary Figs 5D and 6). Finally, we examined whether silencing Dral/FHL-2 would lead to reduced HEK293T cell death. Administration of Dral/FHL-2 siRNA led to a 62% reduction in Dral/FHL-2 protein levels in HEK293T cells as compared to scrambled siRNA controls (Supplementary Figs 5E and F and 6). Following serum withdrawal, we observed a ~50% loss in HEK293T cell survival in control cultures transfected with scrambled siRNA that was rescued in the presence of Dral/FHL-2 siRNA (Fig. 5F).

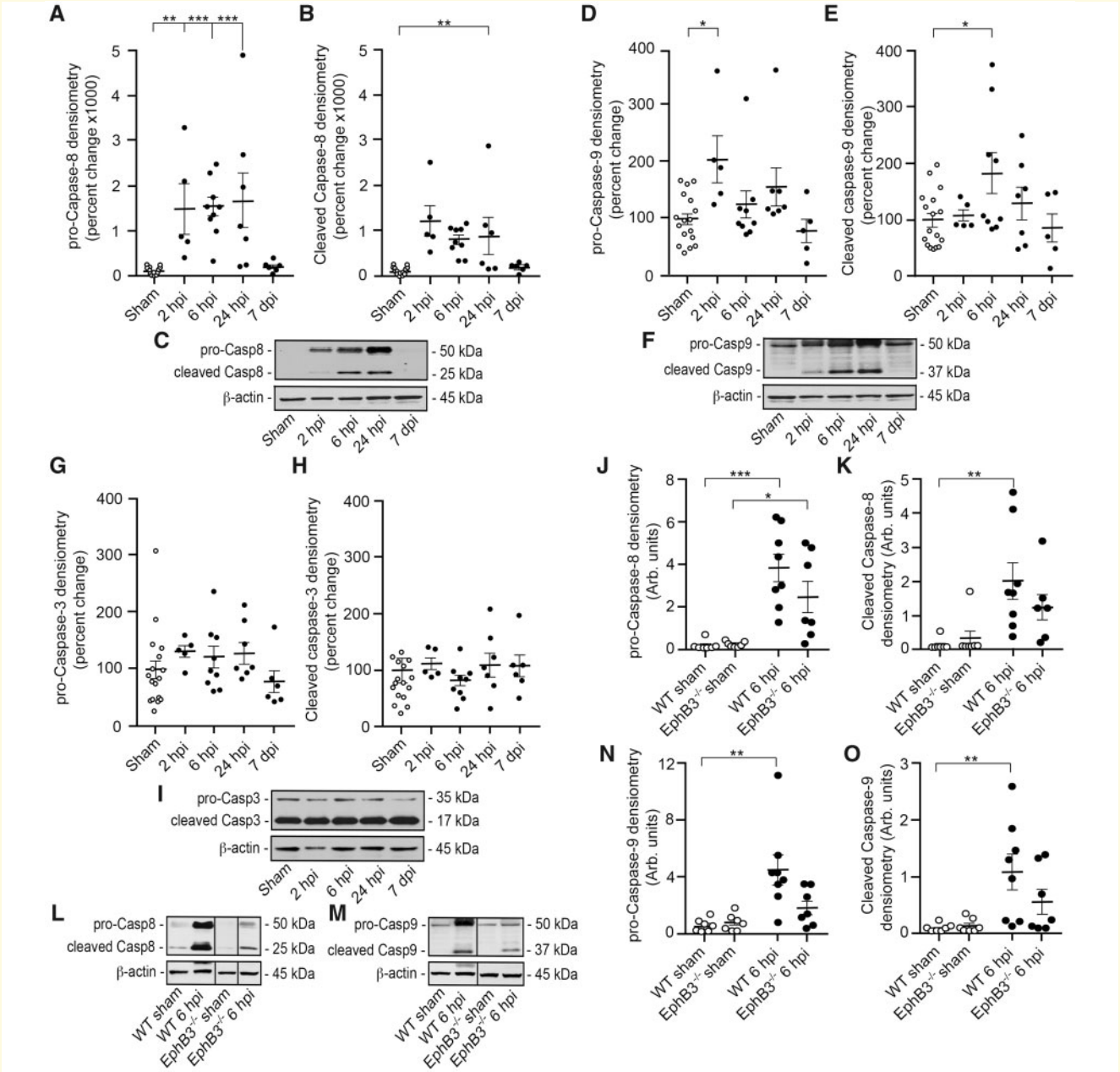

Figure 4 Temporal expression of caspase-8, -9 and -3 demonstrates that the initiator pro- and activated-caspases are significantly increased hours after CCI injury in WT mice but not in EphB3$^{-/-}$ mice. Western blot analysis of pro-caspase-8 (**A**) and cleaved caspase-8 (**B**) shows a significant increase in expression at 2, 6 and 24 hpi that return to baseline by 7 dpi (**C**). Western blot analysis of pro-caspase-9 (**D**) and cleaved caspase-9 (**E**) shows a significant increase in expression at 2, 6 and 24 hpi that return to baseline by 7 dpi (**F**). Western blot analysis of pro-caspase-3 (**G** and **I**) and cleaved caspase-3 (**H** and **I**) shows no significant changes at 2, 6 and 24 hpi as well as 7 dpi. At 6 hpi, WT mice have increased pro- and cleaved caspase-8 (**J**–**L**) and caspase-9 (**M**–**O**), but only pro-caspase-8 was observed to be significantly increased in EphB3$^{-/-}$ mice. *n*-Values were between 6 and 17/group. *$P < 0.05$; **$P < 0.01$; ***$P < 0.01$. Values are presented as mean ± SEM.

Anatomical and functional improvements are observed in the absence of EphB3 after CCI injury

We next determined whether enhanced OL survival in the absence of EphB3 resulted in improved myelin structure, greater axonal conductance and increased behavioural functioning. The number of axons and myelin structure were examined using transmission electron microscopy in WT and EphB3$^{-/-}$ mice at 7 dpi (Fig. 6A and Supplementary Fig. 7A and B). We observed reduced numbers of axons in the corpus callosum between sham

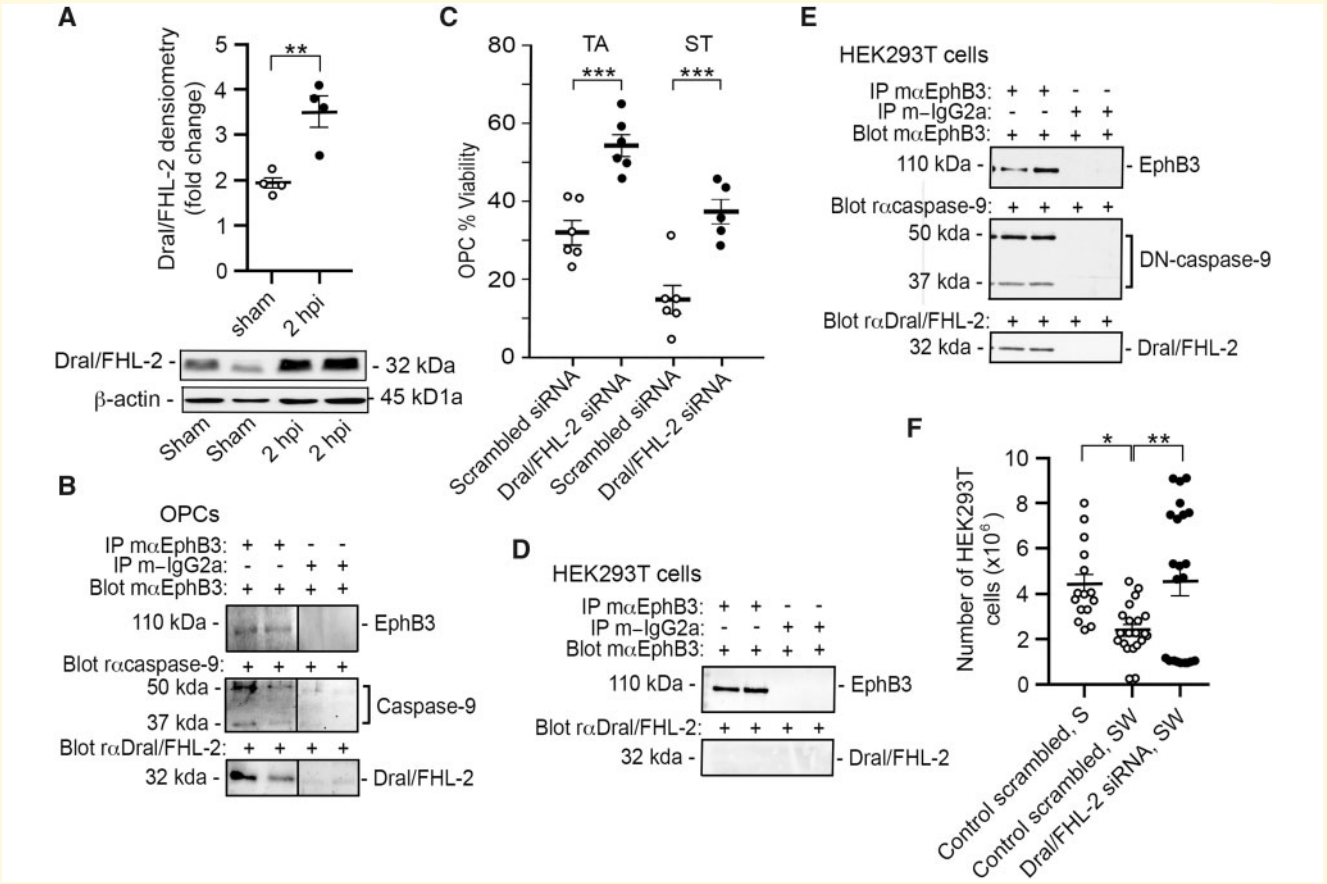

Figure 5 Dral/FHL-2 is up-regulated after brain injury, associates with EphB3 and caspase-9 in primary OPCs and HEK293T cells, and silencing Dral/FHL-2 leads to improved survival. (**A**) Western blot analysis of Dral/FHL-2 at 2 hpi. *n*-Values were 2/group in duplicate. (**B**) IP of Dral/FHL-2 and caspase-9 with anti-EphB3 in primary OPCs. (**C**) Increased survival in Dral/FHL-2 siRNA-treated OPCs after transfection-induced stress (vehicle treatment; TA) and 10 nM ST. (**D**) IP of Dral/FHL-2 is not observed in HEK293T cells transfected with only EphB3. (**E**) IP of Dral/FHL-2 was observed in HEK293T cells transfected with EphB3 and DN-caspase-9. (**F**) Increased survival in Dral/FHL-2 siRNA-treated HEK293T cells after serum withdraw as compared to scrambled siRNA-treated controls and serum controls. $^{*}P < 0.05$; $^{**}P < 0.01$; values are presented as mean ± SEM. mα = mouse antibody; rα = rabbit antibody. DN = dominant-negative; ST = staurosporine treatment; TA = transfection alone.

and CCI-injured mice, although no differences were observed between WT and EphB3$^{-/-}$-injured mice (Fig. 6B and C). Interestingly, we did observe differences in myelin structure between WT and EphB3$^{-/-}$ mice (Fig. 6D). Specifically, WT mice showed increased numbers of collapsed axons/myelin and loosely formed myelin after CCI injury as compared to sham controls, which was not observed in EphB3$^{-/-}$ mice. Regression analysis of G-ratio and axon diameter indicated that WT CCI-injured mice had increased numbers of axons with diameters >3 µm and an increased correlation between reduced myelin in larger diameter axons ($r^2 = 0.53$) as compared to sham controls ($r^2 = 0.03$) (Fig. 6E and G). Conversely, although increased numbers of larger diameter axons were also observed in EphB3$^{-/-}$ mice, there was no correlation between G-ratio and axon diameter in sham and CCI-injured mice (Fig. 6F and H). This is supported by reduced levels of myelin basic protein in WT CCI-injured mice at 7 and 14 dpi, but not in EphB3$^{-/-}$-injured mice (Supplementary Figs 6 and 7C and D).

Axon conductance of the corpus callosum between WT and EphB3$^{-/-}$ mice was also evaluated by measuring evoked CAPs in the corpus callosum at 7 dpi. The evoked callosal CAP consists of biphasic waveforms from short-latency, fast-conducting myelinated axons (N1) and long-latency, slow-conducting unmyelinated axons (N2) (Crawford *et al.*, 2009; Reeves *et al.*, 2012). Input–output responses were generated by gradually increasing stimulus intensity until the N1 response reached asymptotic maximum. The input–output response of both the N1 and N2 components was significantly depressed in WT CCI-injured animals as compared to WT sham animals (Fig. 6I and K and Supplementary Fig. 7E). Analysis of the mean peak amplitude for the N1 and N2 waveforms was likewise decreased after CCI injury (Fig. 6J and L). We further examined whether eliminating EphB3 would

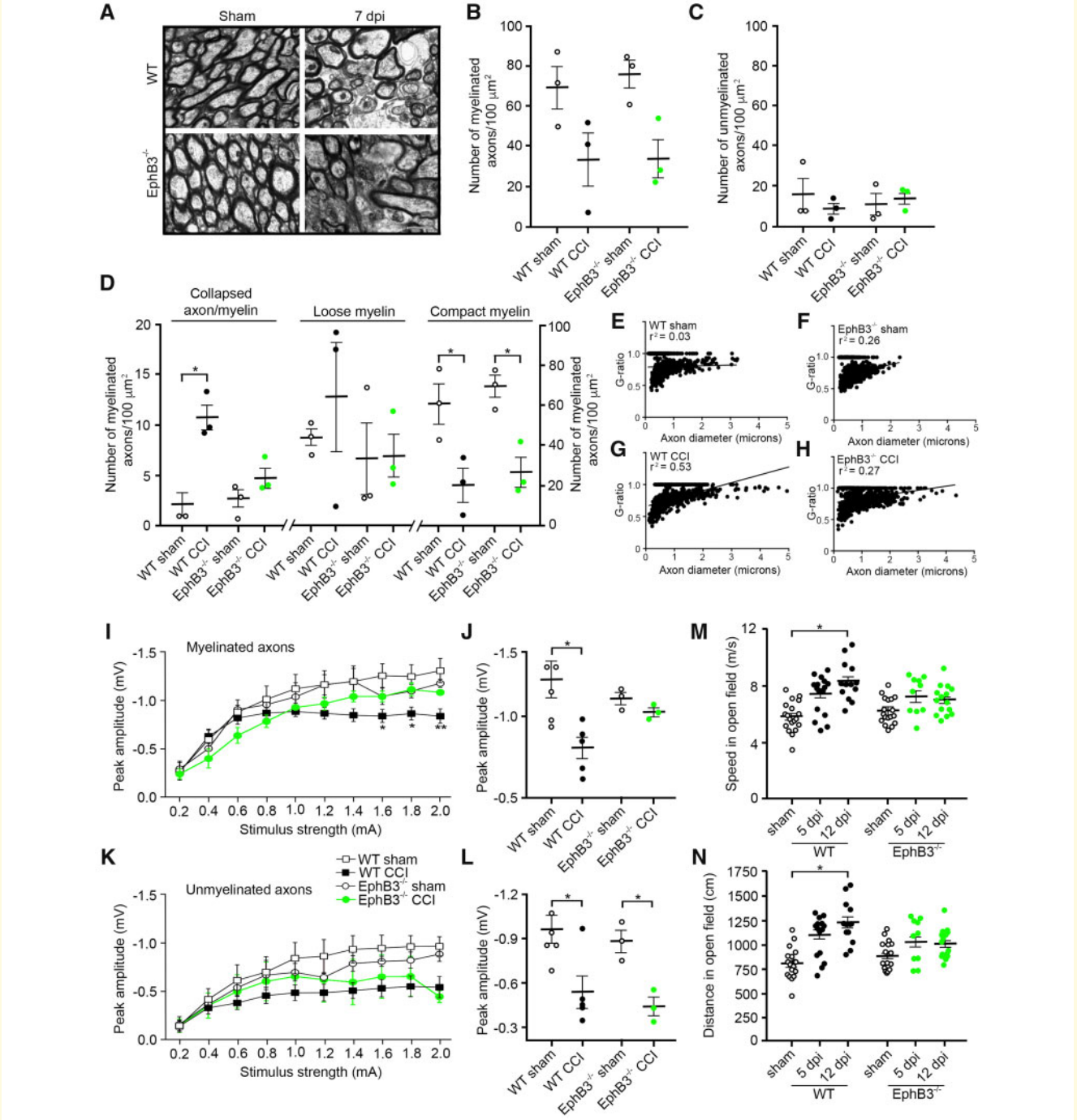

Figure 6 Deficiencies in EphB3 result in reduced myelin damage and improved axonal conductance following CCI injury. (**A**) Transmission electron microscopy of the corpus callosum from WT and EphB3$^{-/-}$ mice at 7 dpi shows reduced numbers of myelinated (**B**) and unmyelinated (**C**) axons in CCI-injured tissues compared to sham. (**D**) Quantification of collapsed axons/myelin, loose myelin and compact myelin shows reduced damage in EphB3$^{-/-}$ mice. *n*-Values were 3/group. (**E**–**H**) Pearson's correlation of the G-ratio to axon diameter suggests that the larger axonal fibres are more susceptible to demyelination following CCI injury in both WT and EphB3$^{-/-}$ mice. Evoked callosal CAP from short-latency, fast-conducting myelinated (N1) axons (**I** and **J**) and long-latency, slow-conducting unmyelinated (N2) axons (**K** and **L**) shows deficits in WT CCI-injured mice. Peak amplitude was measured at 2 mA stimulation (**J** and **L**). *n*-Values were between 3 and 5/group. WT CCI-injured mice exhibit increased hyperactivity responses as compared to WT sham and EphB3$^{-/-}$ mice when measuring speed (**M**) and distance (**N**) in the open field. *$P < 0.05$; **$P < 0.01$. *n*-Values were between 12 and 22/group. Values are presented as mean ± SEM. Bar in (**A**) is 1 μM.

reverse this injury-induced suppression of the evoked CAPs. Interestingly, EphB3$^{-/-}$ reversed the depression of the N1 waveform, but not the N2 waveform (Fig. 6I and K and Supplementary Fig. 7F). Conduction velocity of either the N1 or N2 CAPs was unaltered after CCI injury or in EphB3$^{-/-}$ mice (not shown). These physiological responses are congruent with the EM morphological results and indicate that the improvements in the N1 waveform observed in EphB3$^{-/-}$ mice after CCI injury may be due to the preservation of myelin compaction rather than changes in the number of myelinated axons.

Behavioural testing of motor function is also an important assessment of tissue sparing. Previously, we had shown that CCI-injured EphB3$^{-/-}$ mice and ephrinB3-treated CCI-injured WT mice have improved locomotor function as compared to WT and vehicle controls, respectively, using an activity-based rotarod test (Theus *et al.*, 2014). To determine whether improvements would be observed in a more passive motor test to evaluate spontaneous locomotion, we examined WT and EphB3$^{-/-}$ mice in the open field paradigm at 5 and 12 dpi. Mice, like humans, are known to have a hyperactivity response to TBI that is observable in the open field (Homsi *et al.*, 2010; Biederman *et al.*, 2015). In CCI-injured WT mice, we observed a graded increase in both the speed (Fig. 6M) and distance (Fig. 6N) travelled as compared to sham controls. In the absence of EphB3, this hyperactivity response was not observed. Our findings in the open field together with our previous findings using rotarod analysis suggest that the impaired behavioural motor responses observed after CCI injury can be ameliorated in the absence of EphB3 signalling.

Discussion

Many studies have examined neuron cell death after TBI (Slemmer *et al.*, 2008; Stoica and Faden, 2010); however, fewer studies have aimed to elucidate the mechanisms that regulate OL cell death. The present study implicates a novel 'dependence receptor' mechanism of OL cell death, whereby intracellular cleavage of EphB3 initiates cell death signals in the absence of ligand binding. In the CCI-injured mouse brain, the observed OL cell death was initiated in the cortex and underlying white matter tracts within the first hours after injury with a peak at 6 hpi. The timing of OL loss directly correlated to peak EphB3 cleavage and increased the levels of initiator caspase-8 and -9 in the CCI-injured brain. Reactivation of EphB3 through ephrinB3 administration reversed EphB3 cleavage and OL cell death after CCI injury, which was similar to improved OL survival and functional recovery in EphB3$^{-/-}$ mice. We demonstrated that caspase cleavage of EphB3 requires a multiprotein complex that includes caspase-8 or -9 and Dral/FHL-2, which is up-regulated at 2 hpi, a time period preceding peak EphB3 cleavage. Finally, examination of protein samples from TBI patients showed the presence of both cleaved EphB3 and Dral/FHL-2 in some TBI patients but not in control brain tissues from cardiac patients. Together, our studies define a novel mechanism that regulates OL loss after TBI and identifies potential therapeutic strategies to promote recovery.

OL cell death has been observed in TBI patients as early as 4 hpi, which is a similar time frame to our observed 2–6 hpi OL loss in murine CCI injury. These cellular losses vary depending on the TBI model, species and/or degree of injury. Significant OL losses were observed in rats following fluid percussion injury between 12 hpi and 21 dpi (Conti *et al.*, 1998; Lotocki *et al.*, 2011), while Sullivan *et al.* (2013) reported significant changes in cell density in the corpus callosum at 3 dpi in a murine closed head injury model. In each of these studies, acute time points (<24 h) were not evaluated. Dent *et al.* (2015) used a murine CCI injury model to examine OL numbers between 2 dpi and 3 months post-injury; however, this study primarily focused on the response of immature OLs to differentiate into mature OL. Our studies examined the earliest responses of OL to CCI injury as it relates to both timing of cell loss and differences between specific tissue compartments. Because the mechanical force generated by the pneumatic piston of the CCI injury device may have differential effects on cortical grey matter versus the underlying white matter tracts, we examined these areas separately. We observed differences between OL loss in grey and white matter areas, where tissues with greater tensile strength (i.e. corpus callosum and external capsule) showed peak cell death by 6 hpi, whereas less stiff cortical grey matter areas showed peak losses by 7 dpi. It is also reasonable to consider the possibility that this may reflect differences in energy demands between OLs that reside in white versus grey matter tracts as a result of temporospatial differences in axon myelination, as well as differences in the number and heterogeneity of supporting glial and/or progenitor cells in white and grey matter tissues. Interestingly, white matter regions showed increased OL numbers by 7 dpi, which presumably reflects enhanced OL progenitor differentiation (Dent *et al.*, 2015). OPCs are evident in both white and grey matter areas of the adult CNS where they make up to 5–7% of the glial population (Levine *et al.*, 2001). In the injured or diseased CNS, OPCs become activated to divide and differentiate into mature OLs, contributing to the myelination of demyelinated axons (Dent *et al.*, 2015; Fernandez-Castaneda and Gaultier, 2016; Flygt *et al.*, 2016). Our findings confirm that TBI leads to significant increases in EdU-positive OLs by 7 dpi; however, there were no differences between WT and EphB3$^{-/-}$ mice. This confirms that the greater PLP–GFP counts observed in EphB3$^{-/-}$ tissues as compared to WT tissues result from enhanced OL survival rather than activated oligodendrogenesis.

Our findings demonstrate that the EphB3 receptor plays an important role in regulating OL numbers after

CCI injury through a novel dependence receptor mechanism. Activation of dependence receptors can result from ligand uncoupling leading to intracellular cleavage, exposure of a death domain and activation of downstream pro-apoptotic signals (Mehlen and Bredesen, 2004; Tauszig-Delamasure *et al.*, 2007; Goldschneider and Mehlen, 2010; Theus *et al.*, 2014). Tissue disruption that occurs at the onset of injury can trigger EphB3 cleavage that peaks in OLs by 6 hpi, which coincides with the peak expression of activated initiator caspase-8 and -9. Association of EphB3 with caspase-8 and -9 in brain tissue and primary OPCs strongly supports the role of initiator caspases in receptor cleavage. It is important to note that EphB3-mediated cell death occurring in the traumatically injured CNS may not be limited to OLs, because neural progenitor cells and endothelial cells have also been implicated (Theus *et al.*, 2014; Assis-Nascimento *et al.*, 2018). However, this report is the first to demonstrate a caspase-EphB3 association, *in vivo* receptor cleavage and the requirements of the adaptor protein Dral/FHL-2 to induce cell death. We cannot exclude the possibility that other dependence receptors, including EphA4 receptors (Furne *et al.*, 2009), might also regulate CNS cell survival after brain injury. In fact, EphA4 and EphA7 have been shown to complex with caspase-8 to induce apoptotic cell death (Lee *et al.*, 2015). In short, there are over a dozen known dependence receptors that may represent a novel class of pro-apoptotic molecules in the traumatically injured CNS.

EphB3 cleavage is mediated by a TBI-regulated protein complex that includes the critical adaptor protein Dral/FHL-2. The adaptor protein Dral/FHL-2 and caspase-9 are required for pro-apoptotic activities associated with another dependence receptor (i.e. Patched), where Patched serves as a substrate for a protein complex that includes Dral/FHL-2, TUCAN or NALP1 and caspase-9 (Mille *et al.*, 2009). The murine EphB3 receptor has a single cleavage site at amino acid residue 849, which results in an ~23-kDa fragment that can be detected using a C-terminal anti-EphB3 antibody (Theus *et al.*, 2014). EphB3 may function as a caspase-8 and -9 substrate in both pathological and non-pathological conditions, where the recruitment of other proteins is required to initiate EphB3 cleavage. Dral is a four and a half LIM domain protein 2 (FHL-2) that is thought to regulate protein–protein interactions including the assembly of membrane proteins (Johannessen *et al.*, 2006; Verset et al., 2016). Our studies suggest that EphB3 serves as a substrate for initiator caspases, such as caspase-9, in pathological and non-pathological conditions, but TBI is required for Dral/FHL-2 up-regulation. Dral/FHL-2 associates with EphB3/capase-9 protein complex and leads to casaspe-9-mediated EphB3 cleavage and subsequent initiation of OL cell death. It is reasonable to suggest that Dral/FHL-2 binding in this protein complex is essential for EphB3 cleavage and may provide caspase-9 positional accessibility to enable cleavage to occur. Additional studies are needed to fully characterize this protein cleavage activity associated with dependence receptor actions; however, this protein complex may serve as an important therapeutic target for mitigating cell loss after TBI. Other investigators have implicated the E3 ubiquitin ligase NEDD4 in caspase-9 activation in Patched-mediated apoptosis (Fombonne *et al.*, 2012), which remains to be determined in EphB3-mediated cell death.

There are a number of functional benefits for blocking EphB3 signalling after CNS injury, including improved motor function (Theus *et al.*, 2014; Tsenkina *et al.*, 2015), improved learning and memory (Perez *et al.*, 2016) and reduced TBI-induced hyperactivity. A hyperactivity phenotype has been identified in both experimental TBI models and human TBI patients (Homsi *et al.*, 2010; Adeyemo *et al.*, 2014; Biederman *et al.*, 2015). Hyperactivity is a pathophysiological response primarily due to circuitry disconnection between the cortical and subcortical motor regions that leads to an absence of inhibitory activity (Swanson *et al.*, 1998; Kieling *et al.*, 2008). In the CCI mouse model, the most severely injured tissues include the parietal sensory-motor cortex and the underlying white matter tracts (i.e. corpus callosum and external capsule). More distal tissues, such as the hippocampus and striatum, are also affected but to a lesser extent. It is likely that EphB3-mediated OL cell death plays a major role in the observed functional deficits associated with CCI injury; however, we cannot rule out the possibility that multiple cell types may contribute to the improved behavioural functions associated with EphB3 deletion or ephrinB3 administration. In particular, improved survival of neural progenitor cells and endothelial cells may stabilize the blood–brain barrier and injury microenvironment (Dixon *et al.*, 2016; Assis-Nascimento *et al.*, 2018). We have also shown that EphB3 signalling may have deleterious effects on synaptic stability after TBI, suggesting that decreased EphB3 activity may reduce the global dysfunction of networks in the injured brain (Perez *et al.*, 2016).

Myelination and axonal defects have been associated with all severity levels of TBI, where human post-mortem analysis revealed significant damage years after the initial insult (Flygt *et al.*, 2013; Johnson *et al.*, 2013; Mierzwa *et al.*, 2015). We demonstrate that improved OL survival after CCI injury can also have an important influence on saltatory axonal conduction through stabilization of the myelin sheaths. The deficits observed in the short-latency, fast-conducting N1-evoked CAP at 7 dpi likely reflect the observed differences in collapsed axons and loose myelin associated with CCI-injured WT mice. It is less clear whether these axonal and myelin defects at 7 dpi result from continued EphB3 signalling in surviving OLs or indirectly as a result of acute OL cell loss. Regression analysis of the G-ratio and axon diameter suggests that larger diameter axons are more susceptible to demyelination after CCI injury. In this study, we did observe a significant decrease in the evoked CAP from N2 during

the first week post-injury, but this was not rescued by EphB3 deficiency in mice. This supports previous reports in rat fluid percussion injury models where both myelinated and unmyelinated fibres in the corpus callosum were vulnerable to injury (Reeves *et al.*, 2005; Crawford *et al.*, 2009; Reeves *et al.*, 2012). Taken together, our findings support a molecular machinery for dependence receptor-induced OL cell death after TBI, where EphB3 receptors strongly participate in the pathophysiology of myelin loss after brain injury.

Supplementary material

Supplementary material is available at *Brain Communications* online.

Acknowledgements

The authors thank Maria M Quiala-Acosta, Jose Mier and Maria L. Cepero for technical assistance and animal husbandry, Dr. Melissa M. Carballosa-Gautam for assistance with microscopes and imaging analysis software and Vania Almeida in the Transmission Electron Microscopy Core at the University of Miami Miller School of Medicine. Graphical abstract was generated in BioRender.com.

Funding

This work was supported by the Miami Project to Cure Paralysis, National Institute of Health/National Institute of Neurological Disorders and Stroke [NS098740 (D.J.L.) and NS069721 (C.M.A.)] and the Lois Pope Life Foundation.

Competing interests

There are no conflicts of interest.

References

Adeyemo BO, Biederman J, Zafonte R, Kagan E, Spencer TJ, Uchida M, et al. Mild traumatic brain injury and ADHD: a systematic review of the literature and meta-analysis. J Atten Disord 2014; 18: 576–84.

Ashkenazi A, Dixit VM. Death receptors: signaling and modulation. Science 1998; 281: 1305–8.

Assis-Nascimento P, Tsenkina Y, Liebl DJ. EphB3 signaling induces cortical endothelial cell death and disrupts the blood-brain barrier after traumatic brain injury. Cell Death Dis 2018; 9: 7. https://www.nature.com/articles/s41419-017-0016-5

Biederman J, Feinberg L, Chan J, Adeyemo BO, Woodworth KY, Panis W, et al. Mild traumatic brain injury and attention-deficit hyperactivity disorder in young student athletes. J Nerv Ment Dis 2015; 203: 813–9.

Bigler ED, Burr R, Gale S, Norman M, Kurth S, Blatter D, et al. Day of injury CT scan as an index to pre-injury brain morphology. Brain Inj 1994; 8: 231–8.

Bramlett HM, Dietrich WD. Quantitative structural changes in white and gray matter 1 year following traumatic brain injury in rats. Acta Neuropathol 2002; 103: 607–14.

Bredesen DE, Rao RV, Mehlen P. Cell death in the nervous system. Nature 2006; 443: 796–802.

Casha S, Yu WR, Fehlings MG. Oligodendroglial apoptosis occurs along degenerating axons and is associated with FAS and p75 expression following spinal cord injury in the rat. Neuroscience 2001; 103: 203–18.

Clark RS, Kochanek PM, Watkins SC, Chen M, Dixon CE, Seidberg NA, et al. Caspase-3 mediated neuronal death after traumatic brain injury in rats. J Neurochem 2001; 74: 740–53.

Conti AC, Raghupathi R, Trojanowski JQ, McIntosh TK. Experimental brain injury induces regionally distinct apoptosis during the acute and delayed post-traumatic period. J Neurosci 1998; 18: 5663–72.

Crawford DK, Mangiardi M, Xia X, Lopez-Valdes HE, Tiwari-Woodruff SK. Functional recovery of callosal axons following demyelination: a critical window. Neuroscience 2009; 164: 1407–21.

Dent KA, Christie KJ, Bye N, Basrai HS, Turbic A, Habgood M, et al. Oligodendrocyte birth and death following traumatic brain injury in adult mice. PLoS One 2015; 10: e0121541.

Dixon KJ, Mier J, Gajavelli S, Turbic A, Bullock R, Turnley AM, et al. EphrinB3 restricts endogenous neural stem cell migration after traumatic brain injury. Stem Cell Res 2016; 17: 504–13.

Fernandez-Castaneda A, Gaultier A. Adult oligodendrocyte progenitor cells—multifaceted regulators of the CNS in health and disease. Brain Behav Immun 2016; 57: 1–7.

Flygt J, Djupsjo A, Lenne F, Marklund N. Myelin loss and oligodendrocyte pathology in white matter tracts following traumatic brain injury in the rat. Eur J Neurosci 2013; 38: 2153–65.

Flygt J, Gumucio A, Ingelsson M, Skoglund K, Holm J, Alafuzoff I, et al. Human traumatic brain injury results in oligodendrocyte death and increases the number of oligodendrocyte progenitor cells. J Neuropathol Exp Neurol 2016; 75: 503–15.

Fombonne J, Bissey P-A, Guix C, Sadoul R, Thibert C, Mehlen P. Patched dependence receptor triggers apoptosis through ubiquitination of caspase-9. Proc Natl Acad Sci USA 2012; 109: 10510–5.

Furne C, Ricard J, Cabrera JR, Pays L, Bethea JR, Mehlen P, et al. EphrinB3 is an anti-apoptotic ligand that inhibits the dependence receptor functions of EphA4 receptors during adult neurogenesis. Biochim Biophys Acta 2009; 1793: 231–8.

Fuss B, Mallon B, Phan T, Ohlemeyer C, Kirchhoff F, Nishiyama A, et al. Purification and analysis of in vivo-differentiated oligodendrocytes expressing the green fluorescent protein. Dev Biol 2000; 218: 259–74.

Goldschneider D, Mehlen P. Dependence receptors: a new paradigm in cell signaling and cancer therapy. Oncogene 2010; 29: 1865–82.

Himanen JP, Saha N, Nikolov DB. Cell-cell signaling via Eph receptors and ephrins. Curr Opin Cell Biol 2007; 19: 534–42.

Homsi S, Piaggio T, Croci N, Noble F, Plotkine M, Marchand-Leroux C, et al. Blockade of acute microglial activation by minocycline promotes neuroprotection and reduces locomotor hyperactivity after closed head injury in mice: a twelve-week follow-up study. J Neurotrauma 2010; 27: 911–21.

Johannessen M, Moller S, Hansen T, Moens U, Van Ghelue M. The multifunctional roles of the four-and-a-half-LIM only protein FHL2. Cell Mol Life Sci 2006; 63: 268–84.

Johnson VE, Stewart JE, Begbie FD, Trojanowski JQ, Smith DH, Stewart W. Inflammation and white matter degeneration persist for years after a single traumatic brain injury. Brain 2013; 136: 28–42.

Kabadi SV, Faden AI. Neuroprotective strategies for traumatic brain injury: improving clinical translation. Int J Mol Sci 2014; 15: 1216–36.

Kieling C, Goncalves RR, Tannock R, Castellanos FX. Neurobiology of attention deficit hyperactivity disorder. Child Adolesc Psychiatr Clin N Am 2008; 17: 285–307, viii.

Knoblach SM, Alroy DA, Nikolaeva M, Cernak I, Stoica BA, Faden AI. Caspase inhibitor z-DEVD-fmk attenuates calpain and necrotic cell death in vitro and after traumatic brain injury. J Cereb Blood Flow Metab 2004; 24: 1119–32.

Lee H, Park S, Kang YS, Park S. EphA receptors form a complex with caspase-8 to induce apoptotic cell death. Mol Cells 2015; 38: 349–55.

Levin HS, Williams DH, Valastro M, Eisenberg HM, Crofford MJ, Handel SF. Corpus callosal atrophy following closed head injury: detection with magnetic resonance imaging. J Neurosurg 1990; 73: 77–81.

Levine JM, Reynolds R, Fawcett JW. The oligodendrocyte precursor cell in health and disease. Trends Neurosci 2001; 24: 39–47.

Llambi F, Causeret F, Bloch-Gallego E, Mehlen P. Netrin-1 acts as a survival factor via its receptors UNC5H and DCC. EMBO J 2001; 20: 2715–22.

Llambi F, Lourenco FC, Gozuacik D, Guix C, Pays L, Del Rio G, et al. The dependence receptor UNC5H2 mediates apoptosis through DAP-kinase. EMBO J 2005; 24: 1192–201.

Loane DJ, Faden AI. Neuroprotection for traumatic brain injury: translational challenges and emerging therapeutic strategies. Trends Pharmacol Sci 2010; 31: 596–604.

Lotocki G, de Rivero Vaccari JP, Alonso O, Molano JS, Nixon R, Safavi P, et al. Oligodendrocyte vulnerability following traumatic brain injury in rats. Neurosci Lett 2011; 499: 143–8.

Mehlen P, Bredesen DE. The dependence receptor hypothesis. Apoptosis 2004; 9: 37–49.

Mehlen P, Rabizadeh S, Snipas SJ, Assa-Munt N, Salvesen GS, Bredesen DE. The DCC gene product induces apoptosis by a mechanism requiring receptor proteolysis. Nature 1998; 395: 801–4.

Mierzwa AJ, Marion CM, Sullivan GM, McDaniel DP, Armstrong RC. Components of myelin damage and repair in the progression of white matter pathology after mild traumatic brain injury. J Neuropathol Exp Neurol 2015; 74: 218–32.

Mille F, Thibert C, Fombonne J, Rama N, Guix C, Hayashi H, et al. The Patched dependence receptor triggers apoptosis through a DRAL-caspase-9 complex. Nat Cell Biol 2009; 11: 739–46.

Narayan RK, Michel ME, Ansell B, Baethmann A, Biegon A, Bracken MB, et al. Clinical trials in head injury. J Neurotrauma 2002; 19: 503–57.

Nelersa CM, Barreras H, Runko E, Ricard J, Shi Y, Glass SJ, et al. High-content analysis of proapoptotic EphA4 dependence receptor functions using small-molecule libraries. J Biomol Screen 2012; 17: 785–95.

Nikolov DB, Xu K, Himanen JP. Eph/ephrin recognition and the role of Eph/ephrin clusters in signaling initiation. Biochim Biophys Acta 2013; 1834: 2160–5.

Orioli D, Henkemeyer M, Lemke G, Klein R, Pawson T. Sek4 and Nuk receptors cooperate in guidance of commissural axons and in palate formation. EMBO J 1996; 15: 6035–49.

Perez EJ, Cepero ML, Perez SU, Coyle JT, Sick TJ, Liebl DJ. EphB3 signaling propagates synaptic dysfunction in the traumatic injured brain. Neurobiol Dis 2016; 94: 73–84.

Reeves TM, Phillips LL, Povlishock JT. Myelinated and unmyelinated axons of the corpus callosum differ in vulnerability and functional recovery following traumatic brain injury. Exp Neurol 2005; 196: 126–37.

Reeves TM, Smith TL, Williamson JC, Phillips LL. Unmyelinated axons show selective rostrocaudal pathology in the corpus callosum after traumatic brain injury. J Neuropathol Exp Neurol 2012; 71: 198–210.

Shohami E, Ginis I, Hallenbeck JM. Dual role of tumor necrosis factor alpha in brain injury. Cytokine Growth Factor Rev 1999; 10: 119–30.

Slemmer JE, Zhu C, Landshamer S, Trabold R, Grohm J, Ardeshiri A, et al. Causal role of apoptosis-inducing factor for neuronal cell death following traumatic brain injury. Am J Pathol 2008; 173: 1795–805.

Stoica BA, Faden AI. Cell death mechanisms and modulation in traumatic brain injury. Neurotherapeutics 2010; 7: 3–12.

Sullivan GM, Mierzwa AJ, Kijpaisalratana N, Tang H, Wang Y, Song SK, et al. Oligodendrocyte lineage and subventricular zone response to traumatic axonal injury in the corpus callosum. J Neuropathol Exp Neurol 2013; 72: 1106–25.

Swanson J, Castellanos FX, Murias M, LaHoste G, Kennedy J. Cognitive neuroscience of attention deficit hyperactivity disorder and hyperkinetic disorder. Curr Opin Neurobiol 1998; 8: 263–71.

Tauszig-Delamasure S, Yu LY, Cabrera JR, Bouzas-Rodriguez J, Mermet-Bouvier C, Guix C, et al. The TrkC receptor induces apoptosis when the dependence receptor notion meets the neurotrophin paradigm. Proc Natl Acad Sci USA 2007; 104: 13361–6.

Theus MH, Ricard J, Glass SJ, Travieso LG, Liebl DJ. EphrinB3 blocks EphB3 dependence receptor functions to prevent cell death following traumatic brain injury. Cell Death Dis 2014; 5: e1207. 10.1038/cddis.2014.165.

Tsenkina Y, Ricard J, Runko E, Quiala-Acosta MM, Mier J, Liebl DJ. EphB3 receptors function as dependence receptors to mediate oligodendrocyte cell death following contusive spinal cord injury. Cell Death Dis 2015; 6: e1922. https://www.ncbi.nlm.nih.gov/pmc/articles/PMC4632292/.

Verset L, Feys L, Trepant AL, De Wever O, Demetter P. FHL2: a scaffold protein of carcinogenesis, tumour-stroma interactions and treatment response. Histol Histopathol 2016; 31: 469–78.

World Health Organization. Neurotrauma, 2018. .https://www.who.int/violence_injury_prevention/road_traffic/activities/neurotrauma/en/ (15 October 2020, date last accessed).

Xiong Y, Mahmood A, Chopp M. Emerging treatments for traumatic brain injury. Expert Opin Emerg Drugs 2009; 14: 67–84.